New electrolyte mixture of propylene carbonate and butyltrimethylammonium bis(trifluoromethylsulfonyl)imide (N 1114 TFSI) for high performance silicon nanowire (SiNW)-based supercapacitor applications

Tao Lé, Pascal Gentile, Gerard Bidan, David Aradilla

Research Paper

New electrolyte mixture of propylene carbonate and butyltrimethylammonium bis(trifluoromethylsulfonyl)imide (N_{1114} TFSI) for high performance silicon nanowire (SiNW)-based supercapacitor applications

Tao Lé[a], Pascal Gentile[b], Gérard Bidan[a], David Aradilla[a,*]

[a] Univ. Grenoble Alpes, CEA, CNRS, INAC-SyMMES, F-38000 Grenoble, France
[b] Univ. Grenoble Alpes, CEA, INAC-PhELIQS, F-38000 Grenoble, France

A B S T R A C T

The use of a mixture of propylene carbonate (PC) and N_{1114} TFSI ionic liquid (50:50% w.t) has been investigated as an optimal electrolyte for symmetric micro-supercapacitors based on SiNWs using a large and stable cell voltage of 3.5 V. The device showed an areal capacitance of 150 $\mu F\,cm^{-2}$, an energy density of 1 $mJ\,cm^{-2}$ and a power density of 16 $mW\,cm^{-2}$ maintaining an outstanding cycling stability after $3{\cdot}10^6$ galvanostatic charge-discharge cycles at room temperature. Such properties were comparable to those obtained using the pure ionic liquid. Additionally, the excellent electrochemical performances reported in this study reflect the potential of such mixture to be employed as a promising electrolyte in wide operating temperatures ranging from 0 to 80 °C at large electrochemical windows.

Keywords:
supercapacitors
ionic liquid
electrolyte
mixture
temperature

1. Introduction

In recent years, the research of new electrolytes has awakened an enormous interest in the development of high performance supercapacitors due to their important influences on the electrochemical properties of such devices. Thus, electrolytes play a key role on the cell voltage (V), which is directly related to both energy (E) and power (P) densities, as illustrated in the following equations: $E = 0.5CV^2$ and P^{max}: $V^2/(4ESR)$, where C is the capacitance and ESR is the equivalent series resistance. Within this context, pioneer works reported by Thissandier et al. demonstrated the potential of CVD-grown doped silicon nanowires (SiNWs) to be employed as electrochemical double layer (EDL) capacitive electrode materials in the field of micro-supercapacitors (MSCs) using organic solvent (e.g. a PC solution containing 1 M NEt_4BF_4) [1–3] or ionic liquid (EMIM-TFSI) [4] electrolytes. Precisely, the use of aprotic and protic ionic liquid electrolytes have recently allowed us to improve greatly the electrochemical performances of SiNW-based MSCs due to the synergistic effect produced at the electrode-electrolyte interface using stable and wide cell voltages up to 4 V [5–7]. Consequently, a clear enhancement of the capacitive properties in terms of high power density (182 $mW\,cm^{-2}$), ultra-fast charge-discharge rate (3.5 ms) and extraordinary cycling stability (capacitance retention of 75% after $8{\cdot}10^6$ complete galvanostatic cycles) were achieved in presence of PYR_{13}TFSI electrolyte [5]. In this direction, ionogel electrolytes, as a new tendency in the field of ionic liquids for energy storage devices, based on sol-gel silica with ionic liquid (EMIM TFSI) demonstrated also their potential to withstand solder reflow process (e.g. 280 °C during 40s), which is one of the critical points in the Si-based micro-electronics industry for the integration of components such as micro-supercapacitors [8]. In overall, the performance of SiNW-MSCs using different electrolytes based on organic solvents, ionic liquids or ionogels have attracted a great deal of attention to be integrated as reliable micro-power sources in miniaturized electronic devices [9]. In spite of the excellent results reported in literature, important efforts should be still investigated concerning high voltage electrolytes for MSC applications. In this regard, new strategies focused on mixtures made of organic and nitrile-based solvents with ionic liquid electrolytes [10–12] or eutectic ionic liquids (e.g. PIP_{13}-FSI/PYR_{14}-FSI) [13,14] have emerged as promising alternatives in order to achieve excellent electrochemical performances in carbon-based SCs at a wide range of temperatures Accordingly, to the best of our knowledge, very preliminary results dealing with organic solvent/ionic liquid electrolyte mixtures [e.g. EMIM TFSI (1 M) – PC] were

* Corresponding author.
E-mail address: david.aradilla@cea.fr (D. Aradilla).

addressed to SiNW-based symmetric MSCs [15], demonstrating the potential of such strategy for doped silicon nanostructures in the field of supercapacitors. Therefore, in this work, we present for the first time a complete and exhaustive electrochemical study focused on a new electrolyte mixture (PC-N_{1114} TFSI) to be employed as electrolyte in EDL MSC made of SiNW electrodes able to operate at a wide operating temperature range (0 to 80 °C) within a large cell voltage of 3.5 V. The choice of employing N_{1114} TFSI as electrolyte for the mixture of this study is ascribed to its excellent performance reported in our previous work dealing with SiNWs for supercapacitor devices [16] and its potential also for battery applications [17,18]. Additionally, ammonium structure-based ionic liquids have already demonstrated their enormous potential as electrolytes for carbon supercapacitors [19].

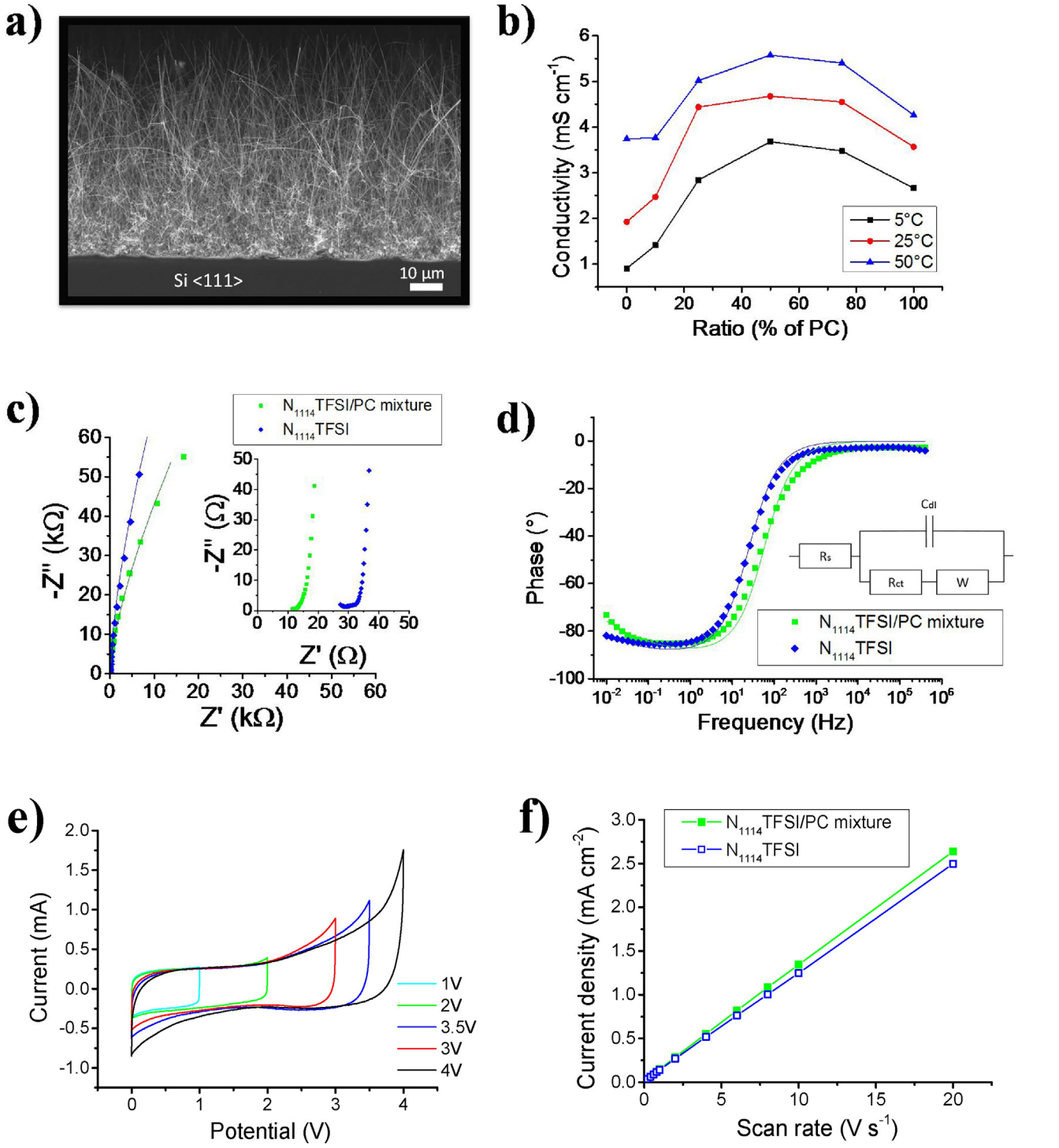

Fig. 1. a) SEM image of SiNWs grown on silicon substrates. b) Conductivity of N_{1114} TFSI as a function of volume percentage in PC. c) Nyquist plot at a frequency range from 400 kHz to 10 mHz for a SiNW-MSC using N_{1114} TFSI (blue diamond) and PC:N_{1114} TFSI (50-50% w.t) (green square) electrolytes. The inset corresponds to the enlarged view of the high frequency region. d) Bode plot of the device obtained from Nyquist plot for N_{1114} TFSI and PC:N_{1114} TFSI (50-50% w.t). Solid lines correspond to the fitting of the experimental data to the equivalent circuit displayed in the inset. e) CV curves of a SiNW-based MSC using different ECWs from 1 to 4 V at a scan rate of 1 Vs^{-1}. f) Current density (j) versus scan rate (ν) for SiNW-based MSCs using PC:N_{1114} TFSI (50-50% w.t) (green line) and N_{1114} TFSI (blue line).

2. Experimental

2.1. Materials and reagents

Round highly p-doped Si (111) substrates (doping level: $5{\cdot}10^{18}$ doping atoms cm^{-3}) and resistivity less than 0.005 Ω cm were used as the substrate for SiNWs growth (Silicon Materials Inc.). Butyltrimethylammonium bis(trifluoromethylsulfonyl)imide (N_{1114} TFSI) and anhydrous propylene carbonate (PC) were purchased from IOLITEC (Ionic Liquids Technologies GmbH, Germany) and Sigma Aldrich. Both chemical reagents were used without further purification. The water content of ionic liquid was determined to be 42 ppm according to our previous work [16].

2.2. Growth of SiNWs

SiNWs were grown in a CVD reactor (EasyTube3000 First Nano, a Division of CVD Equipment Corporation) by using the vapor-liquid-solid (VLS) method via gold catalysis using an optimal procedure reported previously [20]. A SiNWs mass of approximately 750 μg cm^{-2} was estimated according to our previous work [21]. The developed surface (S_{dev}) of SiNWs was calculated using the following equation S_{dev}: $\pi^{*}D^{*}L^{*}d^{*}S_{sample}$, where D is the SiNWs average diameter, L is the length of SiNWs, d is the density of SiNWs and S_{sample} is the sample's plain surface (1.76 cm^2) [3].

2.3. Morphological characterization

The morphology of SiNWs was examined by using a ZEISS Ultra 55 scanning electron microscope operating at an accelerating voltage of 10 kV using a tilt angle of 45°.

2.4. Conductivity measurements

A MMultyConductimeter from MaterialsMates was used to perform conductivity measurements on electrolytes using different ratios of N_{1114} TFSI and PC. The experiments were conducted at 5 °C, 25 °C and 50 °C inside a glove box under a controlled argon environment.

2.5. Electrochemical performance of single electrodes (SiNWs) and micro-supercapacitor devices

The areal capacitance (AC) of single electrodes was evaluated by cyclic voltammetry using a 3-electrode cell configuration employing the corresponding mixtures as electrolyte. SiNWs were employed as working electrode, Pt wire as counter electrode and a Ag/Ag^{+} electrode was used as reference electrode [10^{-2} M silver trifluoromethanesulfonate (AgTf) in a PYR_{13} TFSI solution] [16]. The AC was calculated using the following equation: $AC = Q/(\Delta VA)$, where Q is the average voltammetric charge, which is determined by integrating either the oxidative or reduction scans of the corresponding CV curve, ΔV is the potential range, and A is the geometric surface of the electrode (0.7 cm^2).

SiNW-based (micro)-supercapacitors were built from CR2032 coin cell devices (MSK-160D, MTI, USA) using a symmetric configuration. SiNW electrodes with a diameter of 15 mm in contact with stainless steel disk current collectors were separated by a Whatman separator soaked by the corresponding electrolyte mixture. Cyclic voltammetry (CV) curves, galvanostatic charge-discharge (GCD) cycles and electrochemical impedance spectroscopy (EIS) were performed using a multichannel VMP3 potentiostat/galvanostat with Ec-Lab software (Biologic, France). CV curves were measured at scan rates between 0.1 and 20 V s^{-1} and GCD cycles were performed at current densities between 0.1 and 10 mA cm^{-2}. EIS measurements (Nyquist and Bode plots) were measured using a signal amplitude of 10 mV and a studied frequency range from 400 kHz to 10 mHz. The stability of the coin cells was tested by performing $3{\cdot}10^{6}$ galvanostatic charge-discharge cycles between 0 and 3.5 V at 2.3 mA cm^{-2}. The capacitive properties in terms of AC, energy and power density and coulombic efficiency (η) were calculated using the geometric surface of the electrodes (1.76 cm^2). The AC of the device was evaluated from GCD profiles according to the following formula: $AC = I/A(dV/dt)$, where the I is the discharge current, A is the surface of the electrode and dV/dt corresponds to the slope of discharging curve. The energy (E, μWh cm^{-2}) and power density (P, μW cm^{-2}) values were calculated by using $E = [0.5AC(\Delta V)^2]/3600$ and $P = E/t$, where t is the total time of discharge. The coulombic efficiency (η) was evaluated as the ratio between the discharging and charging times ($\eta = t_d/t_c$) [22]. The corresponding volumetric capacitive properties (E_v and P_v) were calculated taking into account the volume of SiNWs as a cylinder. Thereby, the volume was estimated by the following formula: $V = \frac{D^2\pi}{4}{\cdot}L{\cdot}d{\cdot}A$, where D is the diameter of nanowires (average distribution of approximately 50 nm), L is the length of nanowires (50 μm), d is the density of nanowires ($3{\cdot}10^{9}$ NWs) and A is the geometric surface of the electrode. Based on this approximation, a total volume of $3.2{\cdot}10^{-4}$ cm^3 cm^{-2} was reported. Temperature tests from 20 °C were carried out in an oven using a stabilization time of 4 h to ensure the correct thermalisation of the device. In the case of 0 °C a fridge was employed. All measurements were carried out in an argon-filled glove box with oxygen and water levels less than 1 ppm.

3. Results and discussion

Fig. 1a depicts the cross-sectional view of SiNWs grown on p-doped silicon substrates by CVD. The morphological and structural characterization of SiNW electrodes were already reported in our previous works [7,16,20]. Briefly, doped SiNWs with a length of 50 μm and a diameter range between 20 and 200 nm were estimated. In addition, a density of $3{\cdot}10^{9}$ NWs per cm^2 [20] and a developed surface (S_{dev}) of 920 cm^2 have also reported. Regarding the electrochemical performances no significant differences were observed between type p and n doped SiNWs for supercapacitor applications [1]. Fig. 1b shows the variation of conductivity versus the content of PC in N_{1114} TFSI at different temperatures. As can be seen, the maximal conductivity (σ) was obtained at 50% w.t PC in N_{1114} TFSI for all temperatures. Thus, σ values of 3.7, 4.7 and 5.6 mS. cm^{-1} were obtained at 5 °C, 25 °C and 50 °C respectively. This trend was found in good agreement with similar electrolyte mixture configurations based on PYR_{14}TFSI and nitrile or carbonate solvents (e.g. maximal conductivity values around of 50% w.t) [10]. Particularly, this approach results interesting since the properties of PYR_{14} TFSI, in terms of viscosity (η: 62 mPa s) and conductivity (σ: 2.6 mS cm^{-1}) [23], were found similar to N_{1114} TFSI (η: 95 mPa s and σ: 2 mS cm^{-1}) at room temperature. In this direction, a ratio of 50% w.t using different mixtures of ionic liquids (e.g. PYR_{14} TFSI or Me_3STFSI) and organic solvents (e.g. PC) showed η and σ values close to pure PC containing 1 M Et_4NBF4, which exhibited the highest conductivity and lowest viscosity values by comparison between both the pure ionic liquids and the corresponding mixtures [23,24]. Based on this criteria, this mixture ratio was chosen as an optimal electrolyte for the electrochemical performances reported in this study. EIS technique is a useful tool to evaluate the electrode-electrolyte interface of a SC device. Fig. 1c illustrates the Nyquist plot at a frequency range from 400 kHz to 10 mHz for SiNW-based MSCs using both N_{1114} TFSI and the corresponding optimal mixture electrolyte. The plot shows two important regions at high and low frequency range. At high frequency, the intersection of the semi-circle with the x-axis

represents an ESR value of 11 Ω for the mixture electrolyte, whereas an ESR value of 27 Ω was estimated for pure ionic liquid. This value was found close to another pure ionic liquids, as for example PYR_{13} TFSI (22 Ω) [5] or EMIM TFSI (17 Ω) [7] employing SiNW electrodes. Thus, the decrease of ESR through the dilution of PC in N_{1114} TFSI results a very interesting strategy owing to the increase of conductivity and lower viscosity in mixtures, which represent one of the most important drawbacks for pure ionic liquids [25]. At low frequency, the slight deviation of the vertical line demonstrates the good ionic diffusion and capacitive behaviour predominated by an electrical double layer mechanism. Based on these results, an equivalent circuit was proposed in the inset of Fig. 1d, which was expressed as $R_s[C_{dl}(R_{ct}W)]$, where R_s is the internal resistance of the supercapacitor, C_{dl} is the double layer capacitance, R_{ct} is the charge transfer resistance in serial connection with a Warburg element, W, associated to the diffusion process of the electrolyte ions. EIS technique can also provide an important insight on the electrochemical characterisation of supercapacitor devices by evaluating the relaxation time constant (τ_0), which is defined as the minimum time needed to discharge all the energy from the device with an efficiency of more than 50% [26]. This property was determined from Bode plot (phase angle versus frequency) using the following relation $\tau_0 = 1/f_o$, where f corresponds to the frequency at 45° phase angle [27]. Thus, a τ_0 value of 19.7 ms and 39.5 ms weres calculated for the mixture and pure ionic liquid respectively (Fig. 1d). These values were found similar to those related to SiNW-μSCs using pure ionic liquid electrolytes (e.g. values ranging from 4 ms to 32 ms for EMIM TFSI, PYR_{13}TFSI or NEt_3H TFSI respectively) [4–7]. The determination of an operating electrochemical window (ECW) results also crucial for evaluating the capacitive properties of a supercapacitor device. Fig. 1e displays the CV curves at various ECWs (1, 2, 3, 3.5 and 4 V respectively) at a scan rate of 1 Vs^{-1}. The CV curves reflect a good capacitive behavior with a slight distortion of the profile from 3 V, which was ascribed to silicon oxidation [28]. This effect was evidenced during the first cycles and subsequently a disappearance of the peak was observed due to the passivation of the surface [28]. As a result, wide ECWs up to 4 V evidenced an excellent capacitive behaviour (quasi-ideal rectangular CV shapes) even after long cycling tests [5]. Taking into account this phenomenon, an ECW of 3.5 V was considered as an appropriate cell voltage for further analysis of this study. In order to provide a better comprehension of the importance of such electrolyte mixture, a comparative electrochemical study with pure N_{1114} TFSI ionic liquid was conducted using CV curves. Fig. 1f shows the relationship between the current density (j) and the scan rate (ν) for both electrolytes. The linear regression depicted in the plot demonstrates the predominant effect of a double layer capacitive behaviour. Accordingly, AC values of 0.13 and 0.12 mF cm^{-2} (j = AC ν) were obtained for the mixture and pure ionic liquid electrolytes respectively. This tendency illustrates that the effect of dilution preserves the large electrochemical window (3.5 V) and capacitive properties maintaining an excellent capacitive behaviour even at high scan rates. In this direction, a comparative study concerning different mixture configurations was reported in Fig. 2 using a 3-electrode cell configuration. The CV curves displayed in Fig. 2a reflect the clear enhancement of the stored charge by the optimal 50:50 w.t ratio compared to both the pure ionic liquid and the 90 (PC):10 (N_{1114} TFSI) w.t mixture. This electrochemical behaviour was also analyzed in terms of AC by comparison with other mixtures according to Fig. 2b. As can be seen, the maximal AC value was obtained using the PC-N_{1114} TFSI (50:50% w.t) mixture, which corresponds to the maximal conductivity value (Fig. 1b). This optimal ratio (50:50% w.t) has been widely employed as mixture electrolyte for electrochemical energy storage devices in presence of different ionic liquid chemical structures, as for example

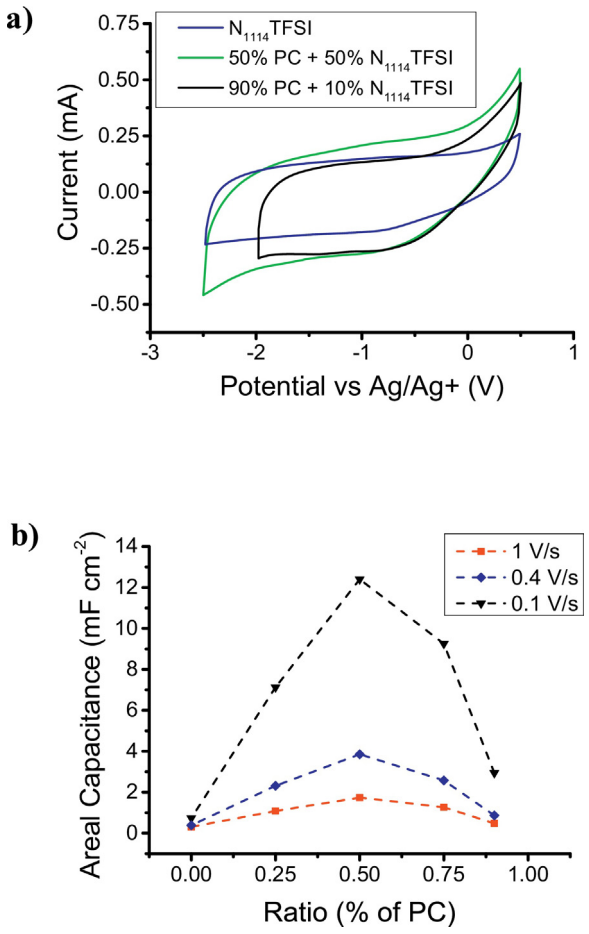

Fig. 2. Electrochemical performance of single electrodes based on hyperbranched SiNWs (silicon nanotrees) under the growth experimental conditions described in Ref. 15. a) CV curves of SiNW electrodes using different electrolyte mixture ratio at a scan rate of 1Vs^{-1}. b) Variation of the AC of SiNWs as a function of the PC volume percentage in N_{1114} TFSI obtained from the CV curves at scan rates of 0.1 Vs^{-1} (black triangle), 0.4 Vs^{-1} (blue diamond) and 1 Vs^{-1} (red square) respectively.

$Me_3NHTFSI$:PC, $PYRNO_3$:PC, Me_3STFSI:PC or $PYR_{14}TFSI$:PC in the field of supercapacitors [29,24,23]. This ratio demonstrated in all the aforementioned cases physical-chemical properties (η and σ) close to pure PC containing salt electrolytes (e.g. NEt_4BF_4) and ECWs larger than 2.7 V (e.g. ECW used commonly for PC containing electrolyte salts). Such characteristics play a key role on the electrochemical performances of supercapacitors since the dilution effect reduces the viscosity, enhaces the diffusion of the ions, which enlarges the ionic conductivity [25,30]. This effect has been demonstrated in the literature by the solvent-solute interaction and solvation effects as the main driving forces to improve the ionic conductivity of the mixtures [10,31].

Fig. 3 shows the electrochemical performance of the SiNW-based micro-supercapacitor using the PC-N_{1114} TFSI (50:50% w.t) mixture at a wide cell voltage of 3.5 V. Fig. 3a shows the galvanostatic charge-discharge cycles at different intensities from 1 to 20 mA. Accordingly, the profiles reflect an excellent reversibility, a good capacitive behaviour as well as an extraordinary fast charge-discharge rate at high current densities (e.g.<10 ms at 20 mA) predominated by an EDL mechanism. The AC was calculated from the discharge profiles displayed in Fig. 3a. Initially, a drop of AC from 0.18 to 0.14 mF cm^{-2} at low current densities ranging from 0.1 to 2.3 mA cm^{-2} was observed (Fig. 3b). This decay was attributed mainly to the surface reactions occurring on SiNWs surface due to the formation of a 1–2 nm nanometric

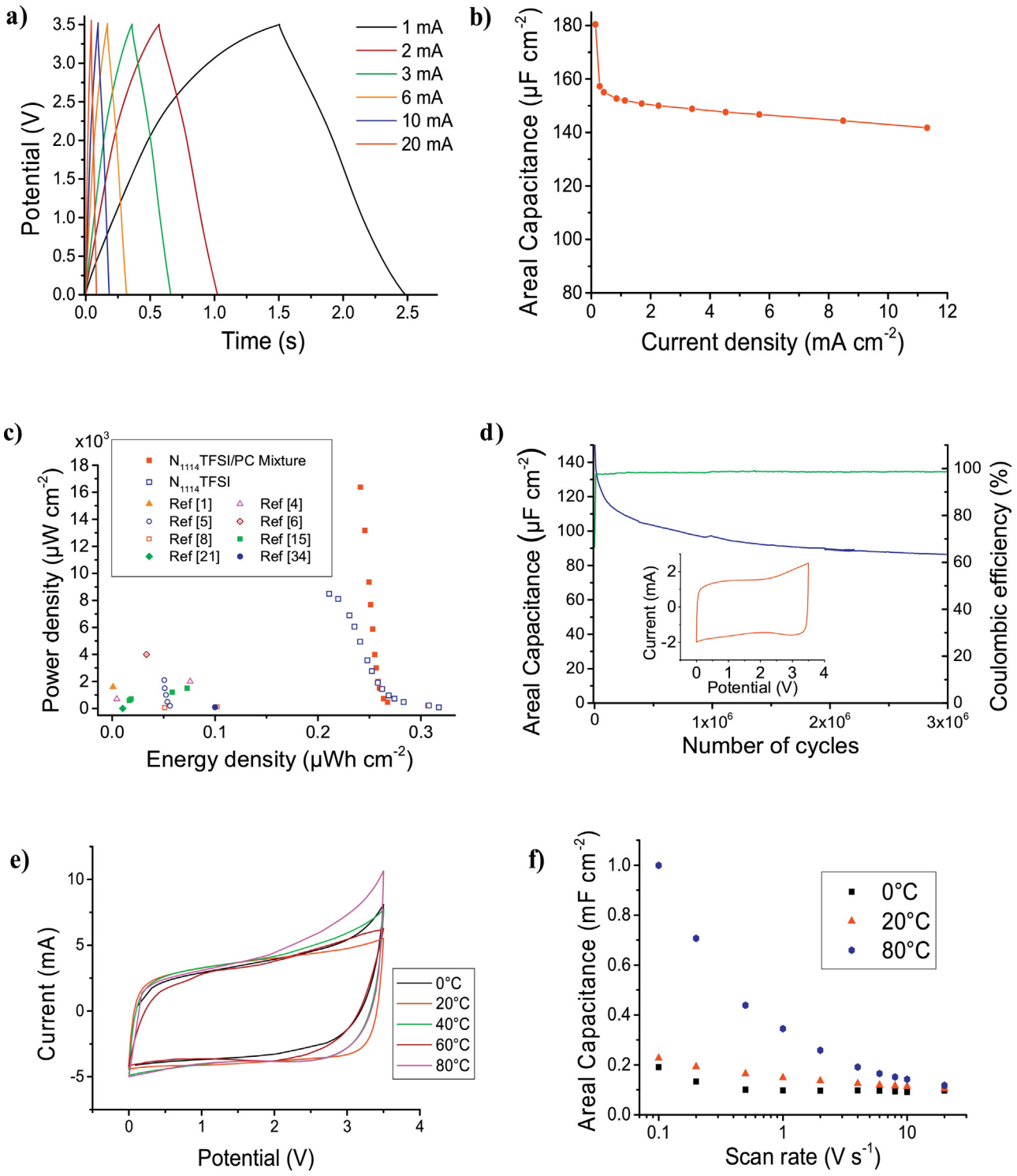

Fig. 3. Electrochemical performance of a symmetric SiNWs-based micro-supercapacitor. a) Galvanostatic charge-discharge cycles at different intensities from 1 to 20 mA. b) Areal capacitance versus current density. c) Ragone plot (P vs E) of the device. The plot shows also the state-of-the-art dealing with previous SiNW-MSCs. d) Cycling stability test (blue line) and coulombic efficiency (green line) over $3{\cdot}10^6$ galvanostatic charge-discharge cycles at a current density of 2.3 mA.cm^{-2}. Inset shows the CV curve after the cycling test at a scan rate of 10 Vs^{-1}. e) CV curves at different operating temperatures ranging from 0 to 80 °C at a scan rate of 20 Vs^{-1}. f) Areal capacitance versus scan rate at different working temperatures, 0 °C (black square), 20 °C (red triangle) and 80 °C (blue circle) respectively.

native silicon oxide layer by the presence of water traces, which was recently confirmed by XPS [32]. Thus, a distortion of the symmetry and linearity of GCD cycles was evidenced because of electrolyte impurities such as halides, surface defects because of inhomogeneous silicon oxidation layer or chemical reactions between SiNW surface and the electrolyte. This electrochemical tendency at low current densities and scan rates was already evidenced in our previous works [5–7]. Subsequently, the device exhibited an AC value of approximately 140 µF cm^{-2} at current densities higher than 2 mA cm^{-2} (Fig. 3b). This value was found higher than the previous results reported in literature concerning SiNW-based MSCs using organic solvent (AC: 7–51 µF cm^{-2},

average values depending on morphological characteristics of SiNWs and electrochemical conditions) [16], ionic liquids ($PYR_{13}TFSI$, AC: 23 $\mu F\,cm^{-2}$ or EMIM TFSI, AC: 13 $\mu F\,cm^{-2}$) [5,33], or ionogels (AC: 60 $\mu F\,cm^{-2}$) [8] electrolytes. This tendency demonstrates the potential of this mixture for micro-supercapacitor applications. Apart from AC, energy and power density are also two key properties to characterize the performance of a supercapacitor device. For that purpose, a Ragone plot (P vs E) was analyzed in Fig. 3c. Power and energy density values were ranged from $0.2{\cdot}10^3$ to $16{\cdot}10^3$ μWcm^{-2} (1.4 to 50.8 $mWcm^{-3}$) and from 0.25 to 0.3 $\mu Whcm^{-2}$ (0.75 to 0.95 $mWhcm^{-3}$) at current densities ranging from 0.1 to 11 $mA.cm^{-2}$ respectively. These values were compared to the state-of-the-art using similar studies dealing with silicon nanostructures such as CVD-SiNWs [1,4–6,8,21], silicon nanotrees (SiNTrs) [15] or silicon carbide nanowires (SiCNWs) [34] in presence of various electrolytes. Additionally, a comparison with other micro-supercapacitors based on the functionalization of CVD-SiNWs by using pseudocapacitive materials such as electroactive conducting polymers (PEDOT and PPy) [35,36] or transition metal oxides (MnO_2) [37] has been also reported. In this direction, as expected according to the working principle of pseudocapacitors, energy density ($2.5 - 5$ $\mu Whcm^{-2}$) was found to be higher than the results reported in this study, whereas the power density ($0.6 - 1{\cdot}10^3$ μWcm^{-2}) was lower compared to pure SiNW EDLCs ($> 2{\cdot}10^3$ μWcm^{-2}) [16]. Consequently, this study reports one of the best electrochemical performances of SiNW-based MSC in terms of AC, E and P thanks to both: (i) the combination of a new configuration device (coin cell), which was never reported before for SiNWs and (ii) the corresponding PC-N_{1114} TFSI electrolyte mixture. The cycling stability is another crucial factor to evaluate the performance of a supercapacitor. From this point of view, the end of life criterion for supercapacitor devices is 20% or 30% loss in capacitance or doubling of the internal resistance [38]. In this work, this property was evaluated by applying $3{\cdot}10^6$ galvanostatic charge-discharge cycles at a current density of 2.3 $mA\,cm^{-2}$. A capacitance retention of 63% was determined after the cycling test with an excellent coulombic efficiency ($\sim$99%) as illustrated in Fig. 3d. The lifetime of the device in this study can be considered as an outstanding value taking into account both the mixture effect and the results reported for pure protic and aprotic ionic liquids with stability values around 70-80% after millions of GCD cycles [4,5,7,8]. Based on the criteria aforementioned, a loss of capacitance of 30% was achieved after 380000 cycles, which can be considered still an excellent result based on EDLCs [39]. Furthermore, an excellent EDL capacitive behavior was kept even after $3{\cdot}10^6$ GCD cycles, as reflected the CV curve in inset in Fig. 3d. Finally, the potential of this device was analyzed at various operating temperatures. Fig. 3e shows the CV curves at 0, 20, 40, 60 and 80 °C using a scan rate of 20 Vs^{-1} at a large cell voltage of 3.5 V respectively. Interestingly, the quasi-ideal rectangular shape of the curves, which corroborates a pure electrochemical double layer capacitive behaviour at a wide range of temperatures from 0 to 80 °C. The variation of AC versus scan rate at different working temperatures is displayed in Fig. 3f. As can be seen, the areal capacitance increases with the temperature leading to values of 94 $\mu F\,cm^{-2}$ (0 °C), 147 $\mu F\,cm^{-2}$ (20 °C) and 344 $\mu F\,cm^{-2}$ (80 °C°) at a scan rate of 1 Vs^{-1}.

4. Conclusions

In summary, the performance of a SiNW-based symmetric supercapacitor device using a coin cell configuration in presence of a PC-N_{1114} TFSI mixture has been successfully demonstrated. The dilution of N_{1114} TFSI in PC at 50% w.t exhibited a maximal conductivity value of 4.7 $mS\,cm^{-1}$ at room temperature, which was used in this study as an optimal electrolyte for electrochemical performances. The device showed a high energy and power density of 1 $mJ\,cm^{-2}$ and 16 $mW\,cm^{-2}$ as well as an outstanding capacitance retention of 63% after $3{\cdot}10^6$ galvanostatic charge-discharge cycles. In addition, a quasi-ideal electrochemical double layer capacitive behaviour was kept at various operating temperatures demonstrating the potential of this device to be employed in a wide range of working temperatures for supercapacitive technological applications.

Acknowledgements

This project has received funding from the European Union's Seventh Program for Research, Technological Development and Demonstration under Grant agreement no. 309143 (NEST Project, 2012 – 2016). B. Iliev and the colleagues from Fraunhofer Institute (Freiburg, Germany) are gratefully acknowledged for providing us the ionic liquid and for cutting the silicon substrates by laser method. The authors would like also thank to Dr. Gutel and Dr. Simone their assistance for the conductivity measurements. Fruitful discussions provided by Prof. Sadki were appreciated. T. Lé acknowledges the Labex-Matisse project and CEA for financial support. This work has been performed with the use of the Hybriden facility at CEA-Grenoble (France).

References

[1] F. Thissandier, A. Le Comte, O. Crosnier, P. Gentile, G. Bidan, E. Hadji, T. Brousse, S. Sadki, Highly doped silicon nanowires based electrodes for micro-electrochemical capacitor applications, Electrochem. Commun. 25 (2012) 109–111.

[2] F. Thissandier, N. Pauc, T. Brousse, P. Gentile, S. Sadki, Micro-ultracapacitors with highly doped silicon nanowires electrodes, Nanoscale Research Letters 8 (2013) 38.

[3] F. Thissandier, P. Gentile, N. Pauc, T. Brousse, G. Bidan, S. Sadki, Tuning silicon nanowires doping level and morphology for highly efficient micro-supercapacitors, Nano Energy 5 (2014) 20–27.

[4] F. Thissandier, L. Dupré, P. Gentile, T. Brousse, G. Bidan, D. Buttard, S. Sadki, Ultra-dense and highly doped SiNWs for micro-supercapacitors electrodes, Electrochim. Acta 117 (2014) 159–163.

[5] D. Aradilla, P. Gentile, G. Bidan, V. Ruiz, P. Gomez-Romero, T. Schubert, H. Sahin, E. Frackowiak, S. Sadki, High performance of symmetric micro-supercapacitors based on silicon nanowires using N-methyl-N-propylpyrrolidinium bis(trifluoromethylsulfonyl)imide as electrolyte, Nano Energy 9 (2014) 273–281.

[6] D. Aradilla, P. Gentile, V. Ruiz, P. Gomez-Romero, J. Wimberg, B. Iliev, T.J.S. Schubert, S. Sadki, G. Bidan, SiNWs-based electrochemical double layer micro-supercapacitors with wide voltage window (4 V) and long cycling stability using a protic ionic liquid electrolyte, Adv. Nat. Sci: Nanosci. Nanotechnol. 6 (2015) 015004–015010.

[7] D. Gaboriau, D. Aradilla, M. Brachet, J. Le Bideau, T. Brousse, G. Bidan, P. Gentile, S. Sadki, Silicon nanowires and nanotrees: Elaboration and optimization of new 3D architectures for high performance on-chip supercapacitors, RSC Adv. 6 (2016) 81017–81027.

[8] M. Brachet, D. Gaboriau, P. Gentile, S. Fantini, G. Bidan, S. Sadki, T. Brousse, J. Le Bideau, Solder-reflow resistant solid state micro-supercapacitors based on ionogels, J. Mater. Chem. A 4 (2016) 11835–11843.

[9] N.A. Kyerematen, T. Brousse, D. Pech, Microsupercapacitors as miniaturized energy-storage components for on-chip electronics, Nat. Nanotechnol. 12 (2017) 7–15.

[10] V. Ruiz, T. Huynh, S.R. Sivakkumar, A.G. Pandolfo, Ionic liquid-solvent mixtures as supercapacitor electrolytes for extreme temperature operation, RSC Adv. 2 (2012) 5591–5598.

[11] C. Schütter, A.R. Neale, P. Wilde, P. Goodrich, C. Hardacre, S. Passerini, J. Jacquemin, A. Balducci, The use of binary mixtrures of 1-butyl-1-methylpyrrolidinium bis{(trifluoromethyl)sulfonyl}imide and aliphatic nitrile solvents as electrolyte for supercapacitors, Electrochim. Acta 220 (2016) 146–155.

[12] S. Leyva-Garcia, D. Lozano-Castello, E. Morallon, T. Vogl, C. Schütter, S. Passerini, A. Balducci, D. Cazorla-Amoros, Electrochemical performance of a superporous activated carbon in ionic liquid-based electrolytes, J. Power Sources 336 (2016) 419–426.

[13] R. Lin, P.-L. Taberna, S. Fantini, V. Presser, C.R. Perez, F. Malbosc, N.L. Rupesinghe, K.B.K. Teo, Y. Gogotsi, P. Simon, Capacitive energy storage from −50 (C to 100 (C using an ionic liquid electrolyte, J. Phys. Chem. Lett. 2 (2011) 2396–2401.

[14] W.-Y. Tsai, R. Lin, S. Murali, L.L. Zhang, J.K. McDonough, R.S. Ruoff, P.-L. Taberna, Y. Gogotsi, P. Simon, Outstanding performance of activated graphene based

supercapacitors in ionic liquid electrolyte from −50 to 80 °C, Nano Energy 2 (2013) 403–411.
[15] F. Thissandier, P. Gentile, T. Brousse, G. Bidan, S. Sadki, Are tomorrow's micro-supercapacitors hidden in a forest of silicon nanotrees? J. Power Sources 269 (2014) 740–746.
[16] D. Aradilla, F. Gao, G. Lewes-Malandrakis, W. Müller-Sebert, P. Gentile, M. Boniface, D. Aldakov, B. Iliev, T.J.S. Schubert, C.E. Nebel, G. Bidan, Designing 3D multihierarchical heteronanostructures for high performance on-chip hybrid supercapacitors: Poly(3,4-ethylenedioxythiophene)-coated diamond/silicon nanowire electrrodes in an aprotic ionic liquid, ACS Appl. Mater. Interfaces 8 (2016) 18069–18077.
[17] V. Chakrapani, F. Rusli, M.A. Filler, P.A. Kohl, Quaternary ammonium ionic liquid electrolyte for a silicon nanowire-based lithium ion battery, J. Phys. Chem. C 115 (2011) 22048–22053.
[18] V. Chakrapani, F. Rusli, M.A. Filler, P.A. Kohl, Silicon nanowire anode: Improved battery life with capacity-limited cycling, J. Power Sources 205 (2012) 433–438.
[19] A. Brandt, J. Pires, M. Anouti, A. Balducci, An investigation about the cycling stability of supercapacitors containing protic ionic liquids as electrolyte components, Electrochim. Acta 108 (2013) 226–231.
[20] D. Aradilla, F. Gao, G. Lewes-Malandrakis, W. Müller-Sebert, D. Gaboriau, P. Gentile, B. Iliev, T. Schubert, S. Sadki, G. Bidan, C.E. Nebel, A step forward into hierarchically nanostructured materials for high performance micro-supercapacitors: Diamond-coated SiNW electrodes in protic ionic liquid electrolyte, Electrochem. Commun. 63 (2016) 34–38.
[21] F. Thissandier, P. Gentile, N. Pauc, E. Hadji, A. Le Comte, O. Crosnier, G. Bidan, S. Sadki, T. Brousse, Highly n-doped silicon nanowires as a possible alternative to carbon for on-chip electrochemical capacitors, Electrochem. 81 (2013) 777–782.
[22] A. Laheäar, P. Przygocki, Q. Abbas, F. Béguin, Appropiate methods for evaluating the efficiency and capacitive behavior of different types of supercapacitors, Electrochem. Commun. 60 (2015) 21–25.
[23] A. Krause, A. Balducci, High voltage electrochemical double layer capacitor containing mixtures of ionic liquids and organic carbonate as electrolytes, Electrochem. Commun. 11 (2011) 814–817.
[24] A. Brandt, C. Ramirez-Castro, M. Anouti, A. Balducci, An investigation about the use of mixtures of sulfonium-based ionic liquids and propylene carbonate as electrolytes for supercapacitors, J. Mater. Chem. A 1 (2013) 12669–12678.
[25] F. Gao, G. Lewes-Malandrakis, M.T. Wolfer, W. Müller-Sebert, P. Gentile, D. Aradilla, T. Schubert, C.E. Nebel, Diamond-coated silicon wires for supercapacitor applications in ionic liquids, Diamond Relat. Mater. 51 (2015) 1–6.
[26] D. Pech, M. Brunet, H. Durou, P. Huang, V. Mochalin, Y. Gogotsi, P.L. Taberna, P. Simon, Ultrahigh-power micrometre-sized supercapacitors based on onion-like carbon, Nat. Nanotechnol. 5 (2010) 651–654.
[27] P.L. Taberna, P. Simon, J.F. Fauvarque, Electrochemical characteristics and impedance spectroscopy studies of carbon-carbon supercapacitors, J. Electrochem. Soc. 150 (2003) A292–A300.
[28] N. Berton, M. Brachet, F. Thissandier, J. Le Bideau, P. Gentile, G. Bidan, T. Brousse, S. Sadki, Wide-voltage-window silicon nanowire electrodes for micro-supercapacitors via electrochemical surface oxidation in ionic liquid electrolyte, Electrochem. Commun. 41 (2014) 31–34.
[29] A. Brandt, J. Pires, M. Anouti, A. Balducci, An investigation about the cycling stability of supercapacitors containing protic ionic liquids as electrolyte components, Electrochim. Acta 108 (2013) 226–231.
[30] D.Y. Kima, J.C. Yang, H.W. Kim, G.M. Swaina, Heterogeneous electron-transfer rate constants for ferrocene and ferrocene carboxylic acid at boron-doped diamond electrodes in a room temperature ionic liquid, Electrochim. Acta 94 (2013) 49–56.
[31] Y. François, K. Zhang, A. Varenne, P. Gareil, New integrated measurement protocol using capillary electrophoresis instrumentation for the determination of viscosity, conductivity and absorbance of ionic liquid-molecular solvent mixtures, Anal. Chim. Acta 562 (2006) 164–170.
[32] D. Gaboriau, M. Boniface, A. Valero, D. Aldakov, T. Brousse, P. Gentile, S. Sadki, Atomic layer deposition alumina-passivated silicon nanowires: Probing the transition from electrochemical double-layer capacitor to electrolytic capacitor, ACS Appl. Mater. Interfaces 9 (2017) 13761–13769.
[33] A. Soam, N. Arya, A. Singh, R. Dusane, Fabrication of silicon nanowires based on-chip micro-supercapacitor, Chem. Phys. Lett. 678 (2017) 46–50.
[34] C.-H. Chang, B. Hsia, J.P. Alper, S. Wang, L.E. Luna, C. Carraro, S.-Y. Lu, R. Maboudian, High-temperature all solid-state microsupercapacitors based on SiC nanowire electrode and YSZ electrolyte, ACS Appl. Mater. Interfaces 7 (2015) 26658–26665.
[35] D. Aradilla, G. Bidan, P. Gentile, P. Weathers, F. Thissandier, V. Ruiz, P. Gomez-Romero, T.J.S. Schubert, H. Sahin, S. Sadki, Novel hybrid micro-supercapacitor based on conducting polymer coated silicon nanowires for electrochemical energy storage, RSC Adv. 4 (2014) 26462–26467.
[36] D. Aradilla, D. Gaboriau, G. Bidan, P. Gentile, M. Boniface, D. Dubal, P. Gomez-Romero, J. Wimberg, T.J.S. Schubert, S. Sadki, An innovative 3-D nanoforest heterostructure made of polypyrrole coated silicon nanotrees for new high performance hybrid micro-supercapacitors, J. Mater. Chem. A 3 (2015) 13978–13985.
[37] D.P. Dubal, D. Aradilla, G. Bidan, P. Gentile, T.J. Schubert, J. Wimberg, S. Sadki, P. Gomez-Romero, 3D hierarchical assembly of ultrathin MnO_2 nanoflakes on silicon nanowires for high performance micro-supercapacitors in Li-doped ionic liquid, Sci. Rep. 5 (2015) 9771.
[38] D. Weingarth, A. Foelske-Schmitz, R. Kötz, Cycle versus holtage hold −Which is the better stability test for electrochemical double layer capacitors? J Power Sources 225 (2013) 84–88.
[39] R. Kötz, M. Carlen, Principles and applications of electrochemical capacitors, Electrochim. Acta 45 (2000) 2483–2498.